



A.P. Beardmore, K. Mukerjee, A.F. Abbey, J.P. Osborne, A. Wells  
University of Leicester, UK

D.N. Burrows, J.E. Hill  
Pennsylvania State University, USA

G. Chincarini, G. Tagliaferri  
Osservatorio Astronomico di Brera, Italy

## Abstract

The X-ray telescope onboard the Swift Gamma-Ray Explorer is designed to make astrometric, photometric and spectroscopic observations of Gamma-Ray Bursts and their associated afterglows in the 0.2-10.0 keV energy band. Automatically switching between four data modes, the XRT CCD camera is able to follow GRB afterglows over a dynamic range of more than seven orders of magnitude in flux. This poster summarises the main properties of the Swift XRT along with the current state of its spectroscopic calibration.

## Introduction

The Swift Gamma-Ray Explorer will make prompt multiwavelength observations of Gamma-Ray Bursts (GRBs) and their associated afterglows. The three instruments (figure 1) are: the Burst Alert Telescope (BAT), which identifies a new GRB; the Optical/UV telescope (UVOT); and the X-ray Telescope (XRT). The observatory aims to measure GRB positions with arcsecond accuracy within 1-2 minutes of their discovery.

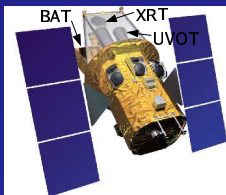


Figure 1: The Swift Gamma-Ray Explorer

## XRT Operating Modes

Due to the dynamic nature of GRBs, and their potentially high initial intensities, the XRT has to be capable of observing over a range of more than seven orders of magnitude in flux. In order to achieve this the XRT operates autonomously and switches between four operating modes depending on the source flux. The modes of operation are:

- **Imaging:** This is a low gain mode (74.2 eV/chan) in which the CCD is operated like an optical device and the photons are allowed to pile-up (i.e. more than one X-ray event per pixel). This mode is invoked when a new GRB target is acquired and is used to calculate the GRB position accurate to 5 arcsecs. The position, and a 'postage stamp' image spanning 50x50 pixels centred on the source, is telemetered to the ground and rapidly distributed through the Gamma-ray burst Coordinate Network (GCN) for follow up observations.
- **Photodiode:** Along with the remaining modes, this is a high gain spectroscopic mode (2.56 eV/chan), but achieves fast timing (0.14 ms resolution) by alternating the parallel and serial readouts one pixel at a time. This means the charge read out from the CCD contains events integrated over the entire field of view and imaging information is lost. However, the GRB will undoubtedly be the brightest source in the field of view. This mode operates when the GRB flux  $F_x$  is  $0.6 \text{ Crabs} < F_x < 60 \text{ Crabs}$ , with pile-up manageable provided  $F_x < 2 \text{ Crabs}$ .

## The X-ray Telescope

The XRT is shown in figure 2. It utilizes flight spare mirrors from the JET-X program, which provide an effective area of  $135 \text{ cm}^2$  at 1.5 keV. These focus incoming X-rays onto a XMM/EPIC MOS CCD22 detector.

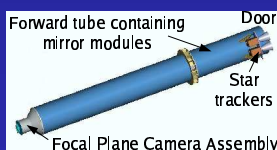


Figure 2: The XRT

The CCD has an image array of  $600 \times 600$  pixels, each of size  $40 \times 40$  microns, which gives a plate scale of 2.36 arcsecs per pixel. The CCD22 type of detector is a front illuminated device but is novel in that it was manufactured with an open electrode structure (figure 3) to enhance its sensitivity to low energy X-rays. It is also made from high resistivity silicon. These enhancements enable it to operate over a bandpass of 0.2 – 10.0 keV.

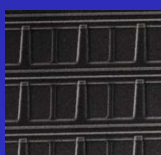


Figure 3: Scanning electron microscope image showing the open electrode structure in a CCD22 device

Fe-55 radioactive sources continuously illuminate a 50 pixel circular diameter region in the corners of the CCD to provide in-flight calibration information.

- **Window Timing:** Another fast timing mode (time resolution 2.2 ms) which is restricted to a central 200 column window. Pixels are further binned by a factor of 10x along columns. 1-D position information is retained. This mode operates when  $1 \text{ mCrabs} < F_x < 600 \text{ mCrabs}$ .
- **Photon Counting:** This is the traditional mode of operation for a X-ray CCD detector, and is used when the flux  $F_x < 1 \text{ mCrab}$ . Full 2-D imaging and spectroscopy is performed with a time resolution of 2.5 secs.

## CCD Calibration

We are modelling the response of the CCD detector to input X-rays with a detailed Monte-Carlo code. The 2-D photon counting simulation includes the following:

- The absorption/transmission of the open electrode structure as a function of position within the pixel.
- A loss function  $f(z)$ , where  $z$  is the active depth

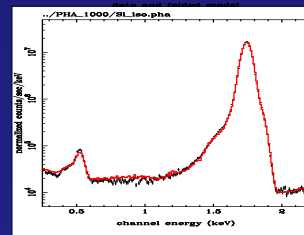


Figure 4: Photon counting Si-Kα calibration data and model fit (red).

below the electrode, to account for surface losses to the front of the detector.

- Charge spreading, which models the radial distribution of the electron cloud as it diffuses towards the electrode structure. This governs the number of pixels the event is detected over, and hence the grade.
- Sub-threshold losses – due to the effects of pixel spreading and noise thresholding, the total energy of the input X-ray event is not always recovered.
- Si fluorescence, which can occur (probability of 4.3%) when an X-ray has an energy greater than the K-shell photoionisation energy of Si. A Si-Kα line (1740 eV) and associated escape peak will be seen in the spectrum provided the fluorescent photon interacts away from the original site.

The window timing and photodiode spectral responses are calculated by translating the 2-D model according to the specific mode of operation.

We are fine tuning the CCD simulator using calibration data taken at Leicester University and the Panter X-ray facility (MPE). Figure 4 shows the results of a spectral fit to photon counting data from a Si-Kα source using the latest RMF - the fit is accurate down to 0.5% of the peak line flux.

## GRB Simulation

Figure 5 shows a simulation of a GRB using the latest photon counting RMF and mirror effective area. The input spectrum was an absorbed power law, with redshifted Fe-Kα line (see figure for the spectral parameters), and the exposure was 30 mins. The Fe-Kα line is clearly detected.

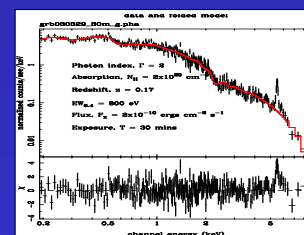


Figure 5: XRT GRB simulation.